J. metamorphic Geol., 2001, **19,** 549–562

Transformation of two-pyroxene hornblende granulite to garnet granulite involving simultaneous melting and fracturing of the lower crust, Fiordland, New Zealand

N. R. DACZKO,[1] G. L. CLARKE[1] AND K. A. KLEPEIS[2]
[1]*School of Geosciences, FO5, University of Sydney, NSW 2006 Australia (ndaczko@mail.usyd.edu.au)*
[2]*Department of Geology, University of Vermont, Burlington, VT 05405, USA*

ABSTRACT Granulite facies gabbroic and dioritic gneisses in the Pembroke Valley, Milford Sound, New Zealand, are cut by vertical and planar garnet reaction zones in rectilinear patterns. In gabbroic gneiss, narrow dykes of anorthositic leucosome are surrounded by fine-grained garnet granulite that replaced the host two-pyroxene hornblende granulite at conditions of 750 °C and 14 kbar. Major and trace element whole-rock geochemical data indicate that recrystallization was mostly isochemical. The anorthositic veins cut contacts between gabbroic gneiss and dioritic gneiss, but change in morphology at the contacts, from the anorthositic vein surrounded by a garnet granulite reaction zone in the gabbroic gneiss, to zones with a septum of coarse-grained garnet surrounded by anorthositic leucosome in the dioritic gneiss. The dioritic gneiss also contains isolated garnet grains enclosed by leucosome, and short planar trains of garnet grains linked by leucosome. Partial melting of the dioritic gneiss, mostly controlled by hornblende breakdown at water-undersaturated conditions, is inferred to have generated the leucosomes. The form of the leucosomes is consistent with melt segregation and transport aided by fracture propagation; limited retrogression suggests considerable melt escape. Dyking and melt escape from the dioritic gneiss are inferred to have propagated fractures into the gabbroic gneiss. The migrating melt scavenged water from the surrounding gabbroic gneiss and induced the limited replacement by garnet granulite.

Key words: fracturing; garnet granulite; lower crust; partial melting; two-pyroxene hornblende granulite.

INTRODUCTION

In this paper, we present structural, metamorphic and geochemical data to establish a mechanism responsible for the simultaneous melting and fracturing of the lower continental crust. Extensive rectilinear, leucosome-filled fracture networks cut gabbroic and dioritic gneiss along a well exposed glacial slab in the Pembroke Granulite near Milford Sound, New Zealand (Blattner, 1976). Adjacent to fractures in the gabbroic gneiss, the host two-pyroxene hornblende granulite assemblage has been replaced by garnet granulite assemblages that reflect conditions involving $T > 750\,^{\circ}C$ and $P \approx 14$ kbar (Clarke *et al.*, 2000). Pods of more fertile dioritic gneiss preserve evidence of partial melting that is inferred to have been controlled by hornblende breakdown at water-undersaturated conditions. Leucosome generated by melting of the dioritic gneiss invaded adjacent, subsolidus gabbroic gneiss. Peritectic garnet porphyroblasts and leucosome in the dioritic gneiss often form elongate trains that parallel leucosome-filled fracture networks in both the gabbroic and dioritic gneiss. Fracture networks are continuous across the dioritic–gabbroic gneiss contacts. These spatial relationships indicate that microfracturing assisted melt segregation in the dioritic gneiss and we infer that millimetre- to centimetre-scale fracturing induced by melt accumulation allowed melt to escape and invade the gabbroic gneiss. Whole-rock geochemical data are presented to show that the partial replacement of two-pyroxene hornblende granulite by garnet granulite was isochemical; it is also inferred that the water-undersaturated melt in the fractures dehydrated the wall rocks to produce the garnet-granulite reaction zones. The Pembroke Granulite preserves a well-exposed example of arrested high-*P* granulite facies metamorphism and evidence for melt-induced fracturing of the lower continental crust.

REGIONAL GEOLOGY

The geology of the south island of New Zealand can be divided into three domains. Eastern and Western Provinces (Landis & Coombs, 1967; Bishop *et al.*, 1985; inset Fig. 1) are separated by a belt of rocks referred to as the Median Tectonic Zone (Kimbrough *et al.*, 1993, 1994; inset Fig. 1) or Median Batholith (Mortimer *et al.*, 1999). Most of the Eastern Province formed by convergent margin processes and contains arc-volcanic rocks, arc-derived sedimentary sequences and accretionary complexes of Permian–Cretaceous age (MacKinnon, 1983; Bradshaw, 1989a; Mortimer,

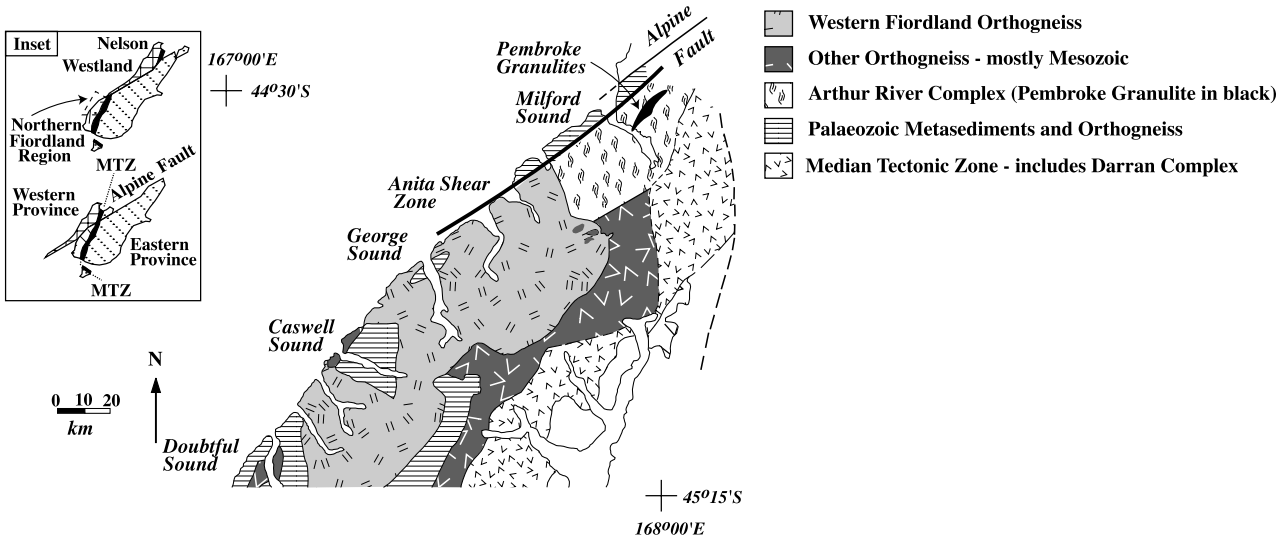

Fig. 1. Geological map of central and northern Fiordland showing major lithological divisions (after Bradshaw, 1990). Inset shows pre-Cenozoic configuration of the South Island, which places the Westland-Nelson region adjacent to Fiordland.

1995). The Western Province contains extensive Lower Palaeozoic metasediments that are cut by Devonian, Carboniferous and Cretaceous granitoids (Muir *et al*., 1996; Wandres *et al*., 1998). Rocks within this province preserve a polyphase mid-Palaeozoic history that occurred when ancestral New Zealand lay within or outboard of the Pacific margin of Gondwana (Wood, 1972; Carter *et al*., 1974; Gibson & Ireland, 1996; Mortimer *et al*., 1999).

The Median Tectonic Zone is a comparatively narrow belt of tectonically disrupted arc-related rocks that includes the Darran Complex in northern Fiordland (Bradshaw, 1993; Kimbrough *et al*., 1993, 1994; Fig. 1). U-Pb zircon ages for rocks of the Median Tectonic Zone mostly fall into two age groups: 247–195 Ma and 157–131 Ma (Kimbrough *et al*., 1994). Late Triassic Median Tectonic Zone plutons that intrude the Eastern Province indicate that these two provinces were together at this time (Williams & Harper, 1978; Mortimer *et al*., 1999). Rocks of the Median Tectonic Zone and the Western Province were intruded by plutons of the 126–105 Ma Western Fiordland Orthogneiss/Separation Point Suite (Bradshaw, 1990; Kimbrough *et al*., 1994; Fig. 1).

The Arthur River Complex (Bradshaw, 1990; Fig. 1) is a belt of granulite facies orthogneiss that lies at the boundary between the Median Tectonic Zone and Western Province rocks in northern Fiordland (Fig. 1). It is heterogeneous in rock-type and structure (Clarke *et al*. 2000) and Mesozoic and Palaeozoic ages have been inferred for orthogneiss units from this belt (Mattinson *et al*., 1986; Bradshaw, 1990). In Milford Sound, the Arthur River Complex includes dioritic gneisses of the Harrison Gneiss and gabbroic gneisses of the Pembroke Granulite and Milford Gneiss (Wood, 1972; Blattner, 1991). The Anita Shear Zone forms the northwestern boundary of the Arthur River Complex; rocks of the Western Province lie north-west of the shear zone (Hill, 1995a, b; Klepeis *et al*., 1999; Fig. 1). The structural relationship between the Arthur River Complex and the Darran Complex (to the east) is less clear, due to most contacts being obscured by vegetation. On the basis of transects made along remote ridges, Blattner (1978, 1991) inferred a gradational transition from hornblende-diorites of the Darran Complex into amphibolites of the Harrison Gneiss and showed that there is no significant chemical difference between the two units. However, other authors have postulated that, in places, regional faults separate the two complexes (e.g. Bradshaw, 1990). An interpretation that at least parts of the Arthur River Complex are rocks of the Median Tectonic Zone that experienced granulite facies metamorphism in the Cretaceous is preferred here (Blattner, 1991), but this interpretation requires confirmation by isotopic dating. The Arthur River Complex is intruded by the Western Fiordland Orthogneiss at its southernmost extent (Bradshaw, 1990; Fig. 1).

Interpretations of the Cretaceous tectonic history of western Fiordland are controversial. Using conventional U-Pb zircon dating (Mattinson *et al*., 1986) and estimates of metamorphic *P–T* paths, Bradshaw (1989b, 1990) and Bradshaw & Kimbrough (1989) inferred a Cretaceous metamorphic history that involved the mid-crustal emplacement of the Western Fiordland Orthogneiss batholith coeval with low- to medium-pressure granulite facies metamorphism. A substantial increase in pressure (*P c.* 6 kbar) and the

subsequent formation of garnet granulite throughout Fiordland was attributed by these authors to tectonic burial consequent to the convergence of arc (Median Tectonic Zone) and continent (Western Province) rocks. Using petrographic and field data presented by Bradshaw (1989b, 1989c, 1990), Oliver (1990) and Brown (1996) inferred that the high–*P* granulite facies conditions were produced by magma loading following emplacement of the Western Fiordland Orthogneiss at mid-crustal conditions. Muir *et al.* (1995, 1998) used geochemical and geochronological data to argue that an early Cretaceous magmatic arc, chemically equivalent to the Darran Complex, was thrust beneath western Fiordland to depths in excess of 40 km and melted to produce the Western Fiordland Orthogneiss. In comparison, Gibson & Ireland (1995), and Ireland & Gibson (1998) inferred that the Western Fiordland Orthogneiss intruded Western Province rocks that were already at lower crustal conditions, and that the Cretaceous history of western Fiordland involved only decompression.

Field and petrographic data for the garnet granulite facies assemblages that occur in planar reaction zones throughout western Fiordland are central to many of these arguments. Garnet granulite is most commonly found in a thin zone either side of anorthositic veins that cut two-pyroxene hornblende-bearing assemblages in the Arthur River Complex and Western Fiordland Orthogneiss (Blattner, 1976; Oliver, 1977; Blattner & Black, 1980; Bradshaw, 1989c). Previous work has focused only on textures in the garnet reaction zones that cut gabbroic gneiss. Blattner (1976) provided a field and petrologic description of the gabbroic gneiss and garnet reaction zones. He used the presence of scapolite in some anorthositic veins to infer that the garnet reaction zones formed in response to an influx of mantle-derived CO_2-rich fluids along a pre-existing joint network. In this model, anorthositic veins, common to the centre of most garnet reaction zones, are unrelated to the garnet reaction zones. Oliver (1977) studied similar garnet reaction zones in the Doubtful Sound region, but proposed an alternative model that involved the partial melting of gabbroic gneiss; melt was inferred to have segregated from the site of production (i.e. a garnet reaction zone) to an adjacent anorthositic vein. Blattner & Black (1980) suggested that volatiles released by hornblende breakdown in gabbroic gneiss of the Pembroke Granulite may have led to melting of plagioclase, to form small proportions of melt as intergranular films. The segregation of these melts may have then contributed to scapolite-bearing anorthositic veins at a structural level above that currently exposed. The interpretations of Blattner & Black (1980) are similar to those of Oliver (1977) in that the garnet reaction zones represent 'restite' or 'melanosome' produced during partial melting. However, Blattner & Black (1980) do suggest that the CO_2 and SO_3 in scapolite must have come from an external source. Bradshaw (1989c) examined garnet reaction zone textures over a wide area of Fiordland, and inferred a two-stage model. He inferred that hornblende-plagioclase veins invaded a network of pre-existing fractures that were subsequently utilised by CO_2-rich fluids that moved along these weaknesses to dehydrate gabbroic gneiss adjacent to the fractures and/or veins.

Excellent exposures in recently deglaciated rocks that experienced only partial replacement of the two-pyroxene hornblende granulite by garnet granulite have led to a good understanding of metamorphic reactions involved in the change from two-pyroxene hornblende-bearing orthogneiss to garnet–clinopyroxene-plagioclase-quartz granulite assemblages (Blattner, 1976; Oliver, 1977; Bradshaw, 1989c). However, the tectonic and metamorphic processes that led to the localised development of garnet granulite have yet to be resolved.

PETROGRAPHY AND FIELD RELATIONS

The Pembroke Granulite (Fig. 1) may be subdivided into gabbroic, dioritic and ultramafic gneiss. Gabbroic gneiss forms the majority of the Pembroke Granulite ($>70\%$ of 0.75 km^2 area studied) and is generally found in the lower reaches of the Pembroke Valley. Dioritic gneiss is generally found in the upper reaches of the Pembroke Valley, but may also crop out as pods within the gabbroic gneiss. Ultramafic gneiss is subordinate to the other two components of the Pembroke Granulite and is generally found as small pods, up to 50 m across, most commonly within the dioritic gneiss. Areas with igneous textures are enveloped by high-strain domains containing S_1 minerals that preserve flaser textures and include deformed grains up to 10 mm in length. Rocks pervasively recrystallized during D1 mostly contain pargasitic hornblende and plagioclase that are elongate in S1.

S1 is variable in orientation and intensity, but generally strikes E to ENE and dips steeply toward the S and SSE. Minerals defining S1 are inferred to reflect conditions of $P<8$ kbar and $T>750$ °C (Clarke *et al.*, 2000). S1 is cut by steeply dipping planar fractures (D2) that are commonly filled by anorthositic veins (Fig. 2a). In domains a few centimetres either side of the fractures and veins, S1 minerals in gabbroic gneiss have been pseudomorphed by garnet, clinopyroxene, quartz and rutile, with or without kyanite. These areas of replacement crop out as distinctive pink alteration bands or what is referred to as a 'garnet reaction zone' (bleached area adjacent to leucosome-filled fractures in Fig. 2a). Garnet–clinopyroxene granulite facies assemblages in the garnet reaction zones record metamorphic conditions of $P\approx14$ kbar and $T>750$ °C (Clarke *et al.*, 2000). Similar reaction zones are not observed adjacent to garnet-bearing leucosome in dioritic gneiss.

Small pods within the gabbroic gneiss that show slight variations in grain size and/or composition may also be cut by anorthositic veins and host garnet reaction zones similar to that in the adjacent

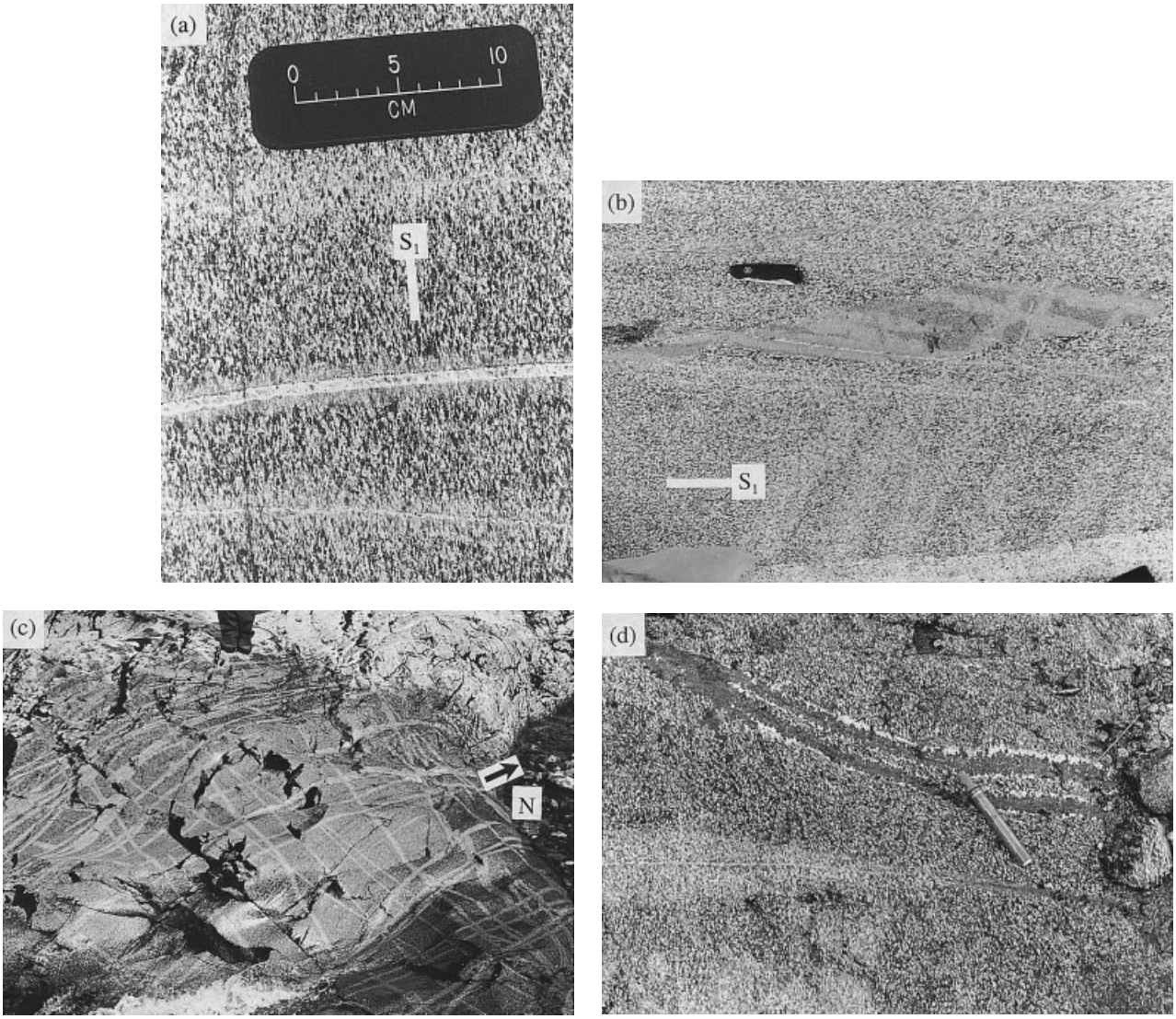

Fig. 2. (a) D2 fractures, commonly filled by anorthositic veins and associated garnet reaction zones, cut S1 in the gabbroic gneiss. Small idioblastic garnet grains at the anorthositic vein/garnet reaction zone boundary are asymmetrically located at the northern side of the centre vein. (b) D2 fractures, anorthositic veins and associated garnet reaction zones, which all cut lithological variations in gabbroic gneiss that are inferred to be igneous. (c) Rectilinear pattern of steeply dipping D2 fractures, anorthositic veins and garnet reaction zones. (d) Contact between gabbroic gneiss (lower left quadrant) and dioritic gneiss (upper and right quadrants). D2 fractures and garnet-bearing leucosomes cut S1 in the dioritic gneiss. The lowermost fracture and garnet-bearing leucosome in the dioritic gneiss (lower right) become an anorthositic vein and garnet reaction zone in the gabbroic gneiss (lower left).

coarser grained gabbroic gneiss (Fig. 2b). These observations indicate that the process forming the garnet–clinopyroxene granulite is strongly related to rock interaction with the D2 fractures and anorthositic veins, and is independent of minor variations in whole-rock composition or grain size. S1 and the garnet reaction zones are variably deformed by east-striking, steeply dipping, narrow ($<$1m wide) mylonite zones (D3) that preserve evidence for sinistral displacement and a well-developed, west-plunging mineral and stretching lineation (L3). Two sets of D4 shear zones cut the D3 mylonites: (1) shallowly south-east-dipping thrusts that have a SE-plunging mineral lineation and top-to-the-NW displacement, and branch into (2) steeply dipping narrow shear zones developed between thrust zones. Metamorphic conditions that accompanied D3 and D4 are inferred to have been $P \approx 14$ kbar and $T \approx 700$ °C (Clarke *et al.*, 2000; Daczko *et al.*, 2001). Detailed discussions of the structural and metamorphic evolution of the Pembroke Granulite are described in Daczko *et al.*, (2000) and Clarke *et al.*, (2000).

Gabbroic Gneiss

The gabbroic gneiss contains elongate and aligned clusters of pargasitic hornblende, orthopyroxene, clinopyroxene, plagioclase, quartz and ilmenite that define a well-developed gneissic S1 foliation (Fig. 2a). Orthopyroxene with exsolution blebs of clinopyroxene or opaque minerals, and clinopyroxene with exsolution blebs of orthopyroxene and opaque minerals, are inferred by us to be relics from an igneous protolith. It is common for clusters of pyroxene to be incompletely mantled by S1 pargasitic hornblende.

The gneissic S1 foliation is cut by a system of anorthositic veins and garnet reaction zones that generally contain two components: (1) a central fracture commonly filled by a garnet-bearing anorthositic vein; and (2) a diffuse garnet-bearing reaction zone that grades into the host gabbroic gneiss (Fig. 2a). Mineral proportions obtained by point counting the different domains are presented in Table 1 (grid references of sample localities are given in Table 2). The anorthositic veins are mostly oligoclase (An_8–An_{31}). The abundance of other minerals in the anorthositic veins is highly variable, but generally $\ll 10\%$ total. Minerals present in small proportions include garnet, kyanite, quartz, hornblende, clinopyroxene and scapolite, although scapolite is generally restricted to larger veins up to 10 cm wide. Scapolite was not found in garnet reaction zone domains, being restricted to the anorthositic veins. Scapolite has crystal form and preserves concentric chemical zoning possibly indicating an igneous origin.

D2 fractures and the garnet reaction zones form a lattice pattern that consists of three sets: east-striking, north-striking, and north-east-striking (Fig. 2c). On the basis of measurements of more than 200 anorthositic veins and associated garnet reaction zones in gabbroic gneiss (*c.* 0.75 km^2 area), the average width of the anorthositic veins is approximately 4 mm and the average width of the anorthositic vein plus garnet reaction zones is approximately 40 mm (Fig. 3). Most anorthositic veins are <5 mm in width, although some veins are up to 30 mm in width. Most garnet reaction zones are 10–50 mm in width, although some reaction zones are up to 100 mm in width. The surface traces of many individual anorthositic veins and garnet reaction zones are continuous and planar for distances in excess of 50 m. Garnet reaction zones in gabbroic gneiss are commonly symmetrically disposed about the anorthositic veins (Fig. 2a). The distance between two reaction zones is commonly <100 mm and the boundaries of some closely spaced garnet reaction zones overlap. Fractures, anorthositic veins and garnet reaction zones cut and slightly offset older fractures, anorthositic veins and garnet reaction zones. This indicates that fracturing, veining and garnet–clinopyroxene granulite formation were synchronous.

Contacts between the anorthositic veins and the garnet reaction zones commonly show interlocking grain boundaries, although some samples preserve a clear microscopic line that defines the original fracture/host gabbroic gneiss contact. Strings of idioblastic garnet grains, up to 5 mm wide, commonly line the margins of the anorthositic veins at contacts with the gabbroic gneiss (Fig. 2a). These garnet grains may define asymmetrical patterns, such that one side of the anorthositic vein may have much more garnet or one side may lack garnet (e.g. upper side of centre vein in Fig. 2a). Two of the sets of garnet reaction zones intersect at approximately 90°; garnet reaction zones

Table 1. Modes of the garnet reaction zone and host gabbroic gneiss for samples 9801 and 9823, obtained by point counting.

Sample	9801 Host	GRZ	9823 Host	GRZ
Grt	0	40	0	40
Plag	34	32	36	32
Qtz	<2	4	<2	2
Amp	40	4	38	2
Cpx	10	10	8	12
Opx	4	0	6	<2
Czo	8	6	10	4
Bt	0	2	0	<2
Rt	0	<2	0	2
Ilm	<2	<2	<2	<2
Total points counted	200	200	200	200

Table 2. New Zealand grid references for samples discussed in text.

Sample	Gneiss Type	NZ grid reference (Milford sheet)
9801	Gabbroic	21044 56120
9808	Dioritic	21043 56123
9814	Gabbroic	21045 56120
9823	Gabbroic	21044 56125
9829B	Dioritic	21043 56124
9834	Gabbroic	21044 56121
9835	Gabbroic	21044 56121

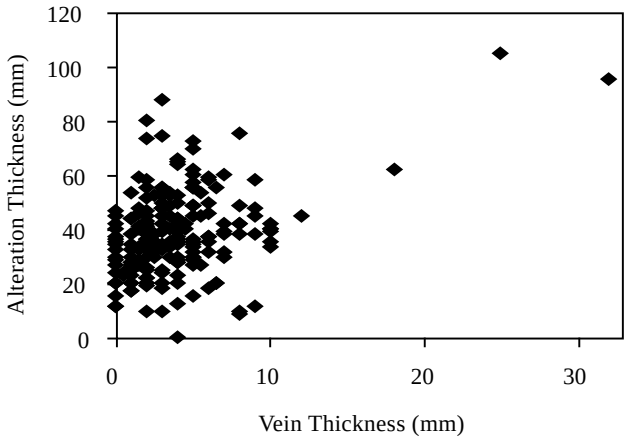

Fig. 3. Plot of anorthositic vein thickness versus garnet reaction zone thickness.

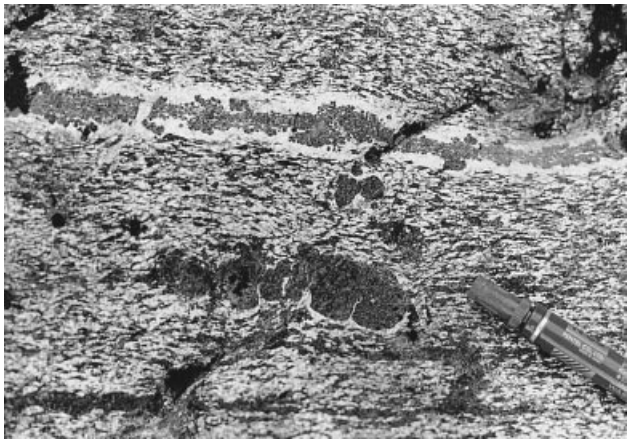

Fig. 4. Garnet poikiloblasts, garnet poikiloblast trains and garnet-bearing leucosome in the dioritic gneiss. The garnet-bearing leucosome/dioritic gneiss contact is undulose, compared with the vein/gabbroic gneiss boundaries in the gabbroic gneiss (Fig. 2a), reflecting a possible rheological contrast between the partially molten dioritic gneiss and solid gabbroic gneiss.

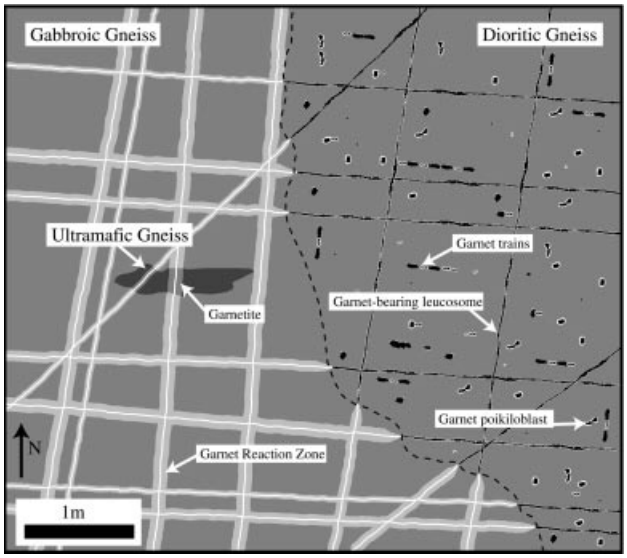

Fig. 5. Cartoon showing how the geometry and style of garnet reaction zones vary across the gabbroic/dioritic gneiss contact. A contrast in the rheology of the partially molten dioritic gneiss and solid gabbroic gneiss appears to have produced little deflection or refraction, as veins traversed the dioritic/gabbroic gneiss boundary. The scale of melt movement is most probably larger than the scale of the diagram.

from the third set intersect the first two at approximately 45°. All D2 fractures and associated veins and garnet reaction zones have steep to near-vertical dips.

Dioritic Gneiss

S1 in the dioritic gneiss is defined by pargasitic hornblende, orthopyroxene, clinopyroxene, biotite, clinozoisite, plagioclase (grains 1–2 mm in diameter), quartz and opaque minerals. This assemblage is similar to that of the gabbroic gneiss, but has more quartz and biotite and less pyroxene. Again, plagioclase is the dominant mineral. The unit contains garnet-bearing leucosomes, some of which are continuous with anorthositic veins that cut gabbroic gneiss (Fig. 2d). However, garnet-bearing leucosomes in the dioritic gneiss do not have garnet reaction zones. Large garnet poikiloblasts up to 10 cm across (Fig. 4), surrounded by plagioclase and quartz, occur through the dioritic gneiss. In places, several garnet poikiloblasts line up to form trains (Fig. 4) enclosed by planar anorthositic veins, which may be aligned with or cut S1. The garnet and the anorthositic veins are inferred to have formed by the incongruent melting of the host rock, as discussed below. Where most extensively developed, these garnet-bearing leucosomes contain two components: (1) a septum of linked garnet poikiloblasts, enclosed by (2) a zone of plagioclase and quartz-bearing leucosome, which is in turn surrounded by the host dioritic gneiss. The large garnet-bearing leucosomes form lattice-like networks similar in size and distribution to those of the anorthositic veins and garnet reaction zones in the gabbroic gneiss. At some localities where dioritic gneiss is in contact with gabbroic gneiss, garnet-bearing leucosomes in the dioritic gneiss change along their length over a distance of a few centimetres into narrow anorthositic veins surrounded by garnet reaction zones in the gabbroic gneiss (Fig. 2d). Figure 5 shows a cartoon representation of the pattern of garnet reaction zones at the boundary between gabbroic and dioritic gneiss. Limited retrogression of the peak assemblage suggests that partial melt has escaped from the dioritic gneiss.

GEOCHEMISTRY

In this section we aim to classify the main rock types in the Pembroke Granulite and to examine the interplay between the host rock, garnet reaction zone and the anorthositic vein in the gabbroic gneiss. Samples were crushed in a hydraulic press and rock fragments, generally <2 cm^3, were separated into vein material (that included garnet porphyroblasts common along vein margins), garnet reaction zone material and host gabbroic gneiss. The diffuse nature of the contact between garnet reaction zone and host gabbroic gneiss generally resulted in the exclusion of small areas of overlap (<2 mm wide). As a result the analyses are a guide to bulk trends in changes in whole-rock composition and may not be strictly representative. Representative samples of dioritic gneiss were crushed without attempting to separate peritectic garnet or leucosome material. The separates were then individually crushed to a fine powder in a tungsten–carbide mill with careful cleaning between samples. Concentrations of the major elements Si, Ti, Al, Fe, Mn, Mg, Ca, Na, K and P and selected trace elements were determined

by Philips PW2400 X-ray fluorescence (XRF) spectrometer at the University of New South Wales, Sydney, Australia, following the procedures of Norrish & Hutton (1969). Whole-rock geochemical analyses of major and trace element concentrations of eight representative samples are presented in Table 3. Additional rare earth elements were determined by instrumental neutron activation analysis (INAA) at the Becquerel Laboratories, Lucas Heights Science and Technology Centre, Sydney, Australia (see Table 3 for list). Sr and Nd isotopic data were obtained at the Centre for Isotope Studies, CSIRO Laboratories, Sydney, Australia, using a VG354 sector thermal ionisation mass spectrometer, and are presented in Table 4.

Table 3. Representative major-oxide and selected trace element data for host gabbroic gneiss, garnet reaction zone and anorthositic vein in samples 9834 and 9835, and dioritic gneiss in samples 9808 and 9829B. Loss of ignition at 1050°C. All concentrations for As, Cd, Mo, Sb, Sn, Th and U are < the lower limit of detection (generally <3 ppm). Rare earth elements by INAA at Becquerel Laboratories, Lucas Heights, Sydney, Australia.

	9835 Gabbroic gneiss	9835 GRZ	9835 Vein	9834 Gabbroic gneiss	9834 GRZ	9834 Vein	9808 Dioritic gneiss	9829B Dioritic gneiss
SiO_2	49.86	49.25	56.69	49.81	50.17	54.14	52.74	54.45
TiO_2	0.97	1.07	0.10	0.91	1.05	0.35	1.06	0.80
Al_2O_3	19.11	19.51	25.80	19.59	19.98	24.29	19.33	19.26
Fe_2O_3*	9.68	10.43	1.25	9.79	10.43	4.07	8.28	8.59
MnO	0.15	0.14	0.02	0.14	0.13	0.07	0.12	0.17
MgO	5.95	6.12	0.61	6.23	6.20	2.31	3.98	4.16
CaO	9.61	9.78	8.50	9.61	9.86	9.10	7.85	7.80
Na_2O	4.47	2.89	6.16	4.13	3.01	5.22	4.83	4.69
K_2O	0.37	0.38	0.30	0.35	0.36	0.33	0.67	0.33
P_2O_5	0.25	0.22	0.06	0.07	0.06	0.08	0.31	0.26
LOI	0.75	0.34	0.54	0.72	0.00	0.68	0.81	0.70
Total	101.17	100.13	100.03	101.35	101.25	100.64	99.98	101.21
XRF (ppm)								
Ba	140	142	110	127	135	106	380	83
Co	46	54	29	52	53	28	38	41
Cr	72	75	<2.9	102	95	4	24	31
Cu	11	20	52	12	19	25	48	87
Ga	20	21	19	20	22	19	20	18
Nb	3	4	2	3	3	2	4	3
Ni	43	45	11	54	56	19	21	23
Pb	8	7	10	8	8	8	12	7
Rb	7	10	13	8	9	13	11	7
Sr	772	774	1381	732	759	1201	855	824
V	269	268	31	236	245	80	194	194
Y	11	12	<2.8	10	11	<2.8	11	8
Zn	89	94	20	88	92	38	95	85
Zr	41	43	59	41	43	52	52	39
INAA (ppm)								
Ce	12.80	12.40	4.12	9.32	9.66	5.00	18.80	15.30
Eu	1.16	1.18	0.34	0.98	1.00	0.56	1.05	1.03
Hf	0.61	0.98	0.33	0.76	0.77	0.31	0.96	0.36
Ho	0.43	0.47	0.15	0.52	0.48	0.27	0.51	0.42
La	5.30	4.76	2.12	3.84	3.50	2.24	8.66	6.57
Lu	0.130	0.130	0.032	0.150	0.140	0.100	0.120	0.120
Nd	8.53	9.01	1.89	7.15	7.26	3.55	11.38	9.48
Sm	2.61	2.86	0.46	2.25	2.51	1.08	2.97	2.30
Ta	<0.50	0.60	0.51	0.57	<0.50	0.52	<0.50	<0.50
Tb	0.40	0.44	0.12	0.40	0.42	0.20	0.48	0.38
Th	<0.20	0.36	<0.20	<0.20	<0.20	<0.20	0.50	0.51
Yb	0.95	0.93	0.26	1.09	1.02	0.71	0.95	0.87

*Total Fe is Fe_2O_3

Rock classification

Two samples of gabbroic gneiss that contain sufficiently large areas of host gneiss, garnet reaction zone and anorthositic vein were collected for whole-rock and isotope analysis. Two additional samples of dioritic gneiss were collected for classification and comparison. The SiO_2 contents of the gabbroic and dioritic gneiss are approximately 49 and 52–54%, respectively. Both rock types have moderate TiO_2 (0.8–1.1%) and Al_2O_3 (19–19.5%) contents, and comparatively high Na_2O (4.1–4.8%) contents. Samples of the anorthositic veins have higher SiO_2 (54–57%) and Al_2O_3 (24–26%) contents. The anorthositic veins are poor in $Fe_2O_3^{total}$ (1–4%), MgO (0.6–2.3%), TiO_2 (0.10–0.35%), and MnO (0.02–0.07%), and have CaO and K_2O contents that are similar to most rocks in the Pembroke Granulite. The P_2O_5 content of the samples of anorthositic vein is very low at *c.* 0.07%, and their Na_2O content is very high at 5–6%.

Comparisons between host gabbroic gneiss, garnet reaction zone and anorthositic vein

The oxide concentration and trace element concentration in garnet reaction zones, from two samples of gabbroic gneiss, were divided by the concentrations in the host gabbroic gneiss, and the ratio of associated enrichment/depletion is shown in Fig. 6. As shown in the figure, there is little difference in SiO_2, MgO, MnO, CaO and K_2O content between the host two-pyroxene hornblende and adjacent garnet–clinopyroxene granulite assemblages. There is a subtle enrichment in TiO_2, $Fe_2O_3^{total}$ and Al_2O_3, and distinct depletion in Na_2O content of the garnet reaction zone, relative to the composition of the host gabbroic gneiss. The loss of Na_2O in the alkali content indicates that metasomatic alteration accompanied formation of the garnet reaction zones, however, it was a minor effect. We do not consider the apparent changes in P_2O_5 to be reliable, due to the small content of P_2O_5 in the gabbroic gneiss and garnet reaction zones (<0.3 wt.%). All trace element contents of the host gabbroic gneiss and garnet reaction zones are similar, except for Cu (Fig. 6). The trace amount of Cu in the host gabbroic gneiss is approximately 11–12 ppm and approximately 19–20 ppm for the garnet reaction zones. Higher trace amounts of Cu (25–50 ppm) are found in the anorthositic veins and dioritic gneiss (*c.* 85–95 ppm). The apparent enrichment of Nb and Rb and depletion of Hf, in sample 9834 is not considered by us to be reliable, due to the small content of these trace elements.

The gabbroic gneiss, dioritic gneiss and anorthositic veins of the Arthur River Complex cannot be discriminated on the basis of measured Sr and Nd isotopic ratios (Table 4). The anorthositic vein material are enriched in Rb and Sr and depleted in Sm and Nd, compared to the gabbroic and dioritic gneisses. Initial

Table 4. Rb-Sr and Sm-Nd isotope data. Rb and Sr concentrations were determined by X-ray fluorescence spectrometer. The $^{87}Sr/^{86}Sr$ composition was measured on a VG354 sector thermal ionisation mass spectrometer at CSIRO, Sydney, Australia. $^{87}Sr/^{86}Sr$ normalised to $^{86}Sr/^{88}Sr = 0.1194$; NBS 987 Sr standard yielded $^{87}Sr/^{86}Sr = 0.710241 \pm 15$ (external precision at $2\sigma = 0.0021\%$, n = 27). $^{87}Rb/^{86}Sr$ ratios calculated from the measured Rb and Sr concentration and $^{87}Sr/^{86}Sr$ ratio. Decay constant used for $^{87}Rb = 1.42 \times 10^{-11}$ a^{-1}. Sm and Nd concentrations were determined by INAA at Becquerel Laboratories, Lucas Heights Science and Technology Centre, Sydney, Australia. The $^{143}Nd/^{144}Nd$ composition was measured on a VG354 sector thermal ionisation mass spectrometer at CSIRO, Sydney, Australia. $^{143}Nd/^{144}Nd$ normalised to $^{146}Nd/^{144}Nd = 0.7219$; O'Nions Nd standard yielded $^{143}Nd/^{144}Nd = 0.511109 \pm 14$ (external precision at $2\sigma = 0.0028\%$, n = 8). $^{147}Sm/^{144}Nd$ ratios calculated from the measured Sm and Nd concentration and $^{143}Nd/^{144}Nd$ ratio. Decay constant used for $^{147}Sm = 6.54 \times 10^{-12}$ a^{-1} and $^{143}Nd/^{144}Nd_{CHUR} = 0.512638$ and $^{147}Sm/^{144}Nd_{CHUR} = 0.1967$. These values were used to calculate initial epsilon values.

Sample	Rb (ppm)	Sr (ppm)	$^{87}Rb/^{86}Sr$	$^{87}Sr/^{86}Sr$	$^{87}Sr/^{86}Sr_i$ 120 Ma	$^{87}Sr/^{86}Sr_i$ 330 Ma	Sm (ppm)	Nd (ppm)	$^{147}Sm/^{144}Nd$	$^{143}Nd/^{144}Nd$	ε_{Nd} 120 Ma	ε_{Nd} 330 Ma
9835 anorthositic vein	13	1381	0.0270	0.703785	0.703739	0.703658	0.46	1.89	0.1471	0.512736	2.7	8.0
9834 anorthositic vein	13	1201	0.0311	0.703756	0.703703	0.703610	1.08	3.55	0.1839	0.512763	2.6	7.9
9835 gabbroic gneiss	7	772	0.0261	0.703788	0.703743	0.703665	2.61	8.53	0.1849	0.512753	−2.5	2.7
9834 gabbroic gneiss	8	732	0.0314	0.703842	0.703788	0.703695	2.25	7.15	0.1902	0.512781	−2.2	3.1
9829B dioritic gneiss	7	824	0.0244	0.703840	0.703798	0.703725	2.30	9.48	0.1466	0.512745	−1.1	4.2
9808 dioritic gneiss	11	855	0.0370	0.703816	0.703753	0.703642	2.97	11.38	0.1577	0.512776	−0.9	4.3

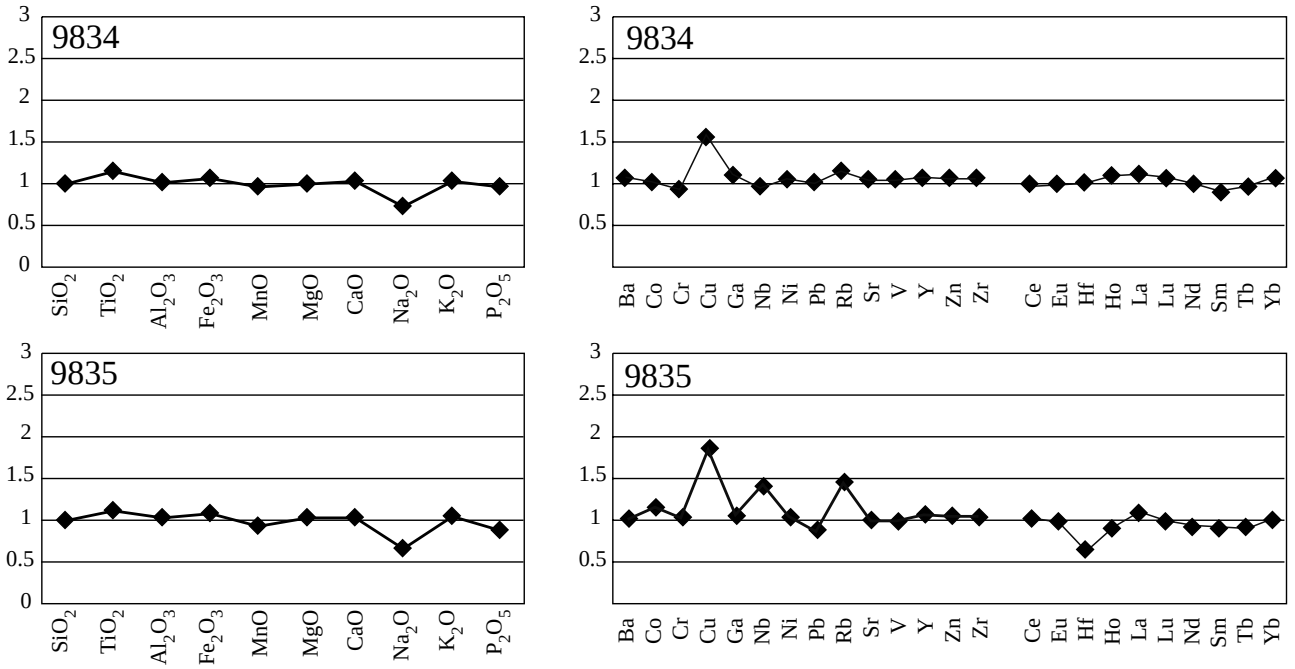

Fig. 6. Major oxide and trace element concentration ratios of garnet reaction zone versus host gabbroic gneiss for samples 9834 and 9835. Points that plot near to one indicate essentially isochemical behaviour for that element. A number greater than one indicates enrichment of that element in the garnet reaction zone and a number less than one indicates depletion.

Sr isotope ratios and ε_{Nd} values have been calculated for arbitrary initial ages of 330 Ma and 120 Ma, to account for the limited constraint of protolith age and timing of partial melting (Bradshaw, 1990). The low $^{87}Sr/^{86}Sr$ initial ratio points to a mantle or lower crustal origin for the gabbroic and dioritic protoliths. The low radiogenic Sr isotopic composition of all samples suggests no contamination by a more evolved crustal component. The range of ε_{Nd} values suggest that the anorthositic vein material is much younger than the host rock, consistent with a Palaeozoic age for the host gneisses and a Cretaceous age for the partial melting that is inferred to have produced the anorthositic veins. However, these interpretations need confirmation by well-constrained isotopic dating.

Garnet and rutile are absent from gabbroic gneiss that encloses the garnet reaction zones. Orthopyroxene and hornblende are mostly absent from the inner garnet reaction zones, whereas they are common in the host gabbroic gneiss and in outer parts of the garnet

reaction zone (near the diffuse garnet reaction zone/host gabbroic gneiss boundary). Clinopyroxene, plagioclase, quartz and opaque minerals are present in both areas. Plagioclase is less abundant in the garnet reaction zones than in the host gabbroic gneiss. As discussed below, the gabbroic gneiss shows small grains of kyanite in plagioclase. Modal clinopyroxene and quartz increase with the transformation of host gabbroic gneiss to garnet reaction zone. Thus, the two-pyroxene hornblende granulite to garnet–clinopyroxene granulite transformation involves the breakdown of orthopyroxene and hornblende, in the presence of plagioclase, to form garnet, clinopyroxene and quartz, and the breakdown of ilmenite to form rutile. The following reaction approximates the transformation (see also Blattner, 1976; Oliver, 1977; Bradshaw, 1989c):

$$\text{Prg-Hb} + \text{Opx} + \text{Plag} \rightarrow \text{Grt} + \text{Cpx} + \text{Qtz} + \text{H}_2\text{O} \quad (1)$$

As reaction (1) is principally pressure-dependent, the change is consistent with burial of the Pembroke Granulite. The change has been modelled in CNFMASH (CaO–Na_2O–FeO–MgO–Al_2O_3–SiO_2–H_2O), using THERMOCALC (v2.6) and the '20 April 1996' internally consistent thermodynamic data set (Powell *et al.*, 1998), and indicates a change in conditions from $P<8$ to $P\approx14$ kbar (Clarke *et al.*, 2000).

Comparisons with previous work

With the exception of decreased Na_2O content, the garnet reaction zones in the Pembroke Granulite have the same bulk geochemistry as the host gabbroic gneiss. In this section, we combine our representative geochemical data with data published by Blattner (1976), Oliver (1977) and Bradshaw (1989c), for the purpose of comparing the garnet reaction zones in the Pembroke Granulite (Blattner, 1976; this study) with those studied in the Western Fiordland Orthogneiss (Oliver, 1977; Bradshaw, 1989c). Garnet reaction zones described from the Western Fiordland Orthogneiss are similar to those described above for the gabbroic gneiss in the Pembroke Valley. Figure 7 shows compiled data plotted on Peacock and Al saturation index (ASI) diagrams, after Brown (1982) and Zen (1986) respectively. A consistent calc-alkaline trend can be observed for the combined data set. Tie lines drawn between all paired host rock and garnet reaction zone points indicate that the garnet reaction zones are slightly less metaluminous (ASI 0.90–0.95) compared to the adjacent host rocks (ASI 0.75–0.80). The anorthositic veins straddle the boundary between the peraluminous and metaluminous classification (ASI 1). The systematic trend is consistent with all the Fiordland garnet reaction zones having formed by a similar process.

QUANTITATIVE CATION MAPPING

In this section we examine in detail the interplay between host rock and garnet reaction zone in the gabbroic gneiss using quantitative cation maps. The determination of the number of cations of Si, Al, Fe, Mn, Mg, Ca, Na and K for 24 oxygens was completed by first collecting raw intensity X-ray maps using a

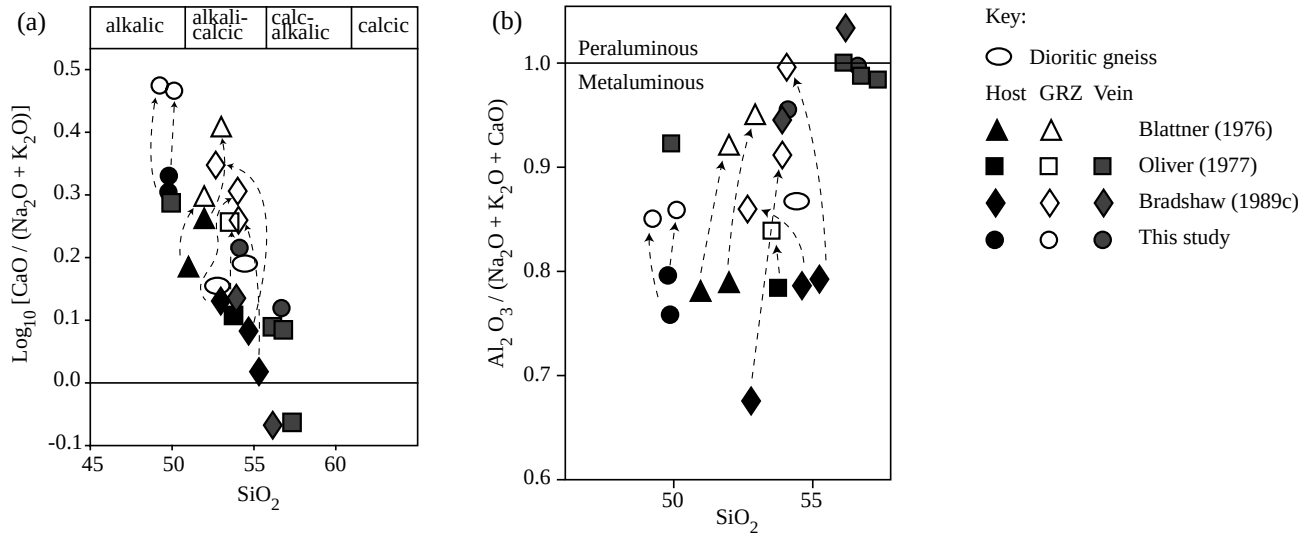

Fig. 7. (a) Peacock Index diagram (after Brown, 1982). The Peacock Index for a particular rock suite is calculated from the point where the data trend crosses the zero $\log_{10}$ [$CaO/(Na_2O+K_2O)$] value. Dashed lines with arrows indicate the change from host gabbroic gneiss (filled shapes) to garnet reaction zone (open shapes). Grey-filled shapes indicate the composition of the anorthositic veins. Oval shapes represent the dioritic gneiss. (b) Aluminium Saturation Index (Zen, 1986). Plot of mol. $Al_2O_3/(CaO+Na_2O+K_2O)$ versus SiO_2. Samples of garnet reaction zone are slightly less metaluminous than the adjacent host gabbroic gneiss.

Cameca SX50 microprobe at the University of New South Wales with an accelerating voltage of 15 kV and a beam width of 1–3 μm. We collected a 3.5 cm by 2.5 mm map that traversed the anorthositic vein/garnet reaction zone boundary and the garnet reaction zone/host gabbroic gneiss boundary in gabbroic gneiss sample 9814. This map was collected with a 70 ms count time at each point and a 10 μm step size between points. The raw intensity maps were converted to maps of oxide wt % by using the α-factor approach of Bence & Albee (1968) for matrix correction (G.L. Clarke *et al*., in press). The matrix-corrected data were then recalculated for 24 oxygens to give cation proportions. Appropriate threshold values of cation proportions were then used to calculate mineral modes.

The cation map was analysed to determine modes across the transition from two-pyroxene hornblende granulite to garnet–clinopyroxene granulite. The map was initially divided into garnet reaction zone and host gabbroic gneiss. Table 5 presents the modes determined for this analysis. Minor minerals, such as kyanite (<1 vol.%) and apatite (<2 vol.%), occur in approximately the same proportions in the garnet reaction zone as in the host gabbroic gneiss. Other minerals present in small proportions, such as quartz and clinozoisite are rare in the host gabbroic gneiss and increase to greater than 1 vol.% in the garnet reaction zone. The plagioclase mode decreases from 56 vol.% in the host gabbroic gneiss to 51 vol.% in the garnet reaction zone. Related to this is an increase in the total mode of the main mafic minerals (garnet, clinopyroxene and hornblende) from 42 vol.% in the host gabbroic gneiss to 45 vol.% in the garnet reaction zone. The 12 vol.% hornblende mode in the garnet reaction zone represents the incomplete replacement of S1 hornblende at the margins of the garnet reaction zone.

So as to examine the garnet reaction zone/host gabbroic gneiss boundary, the cation map was divided into many smaller equally sized areas and analysed to determine if there was any systematic change in modes across the garnet reaction zone/host gabbroic gneiss boundary. The change in plagioclase mode between the two areas is approximately 4 vol.%. This change was too small to examine graphically across the two zones so it was not possible to determine whether the mode of plagioclase was depleted most near the garnet reaction zone/host gabbroic gneiss boundary or near the garnet reaction zone/anorthositic vein boundary. However, the modes of minerals such as quartz, garnet, clinopyroxene and hornblende show systematic trends across the transition.

Table 5. Modes of gabbroic gneiss sample 9814, determined by image analysis of cation maps.

	Host	GRZ	Vein
Ky	0.9	0.7	0.2
Qtz	0.0	1.8	1.8
Ap	1.5	0.7	0
Plag	55.5	50.6	92.5
Czo	0.0	1.2	2.8
Gr	0.0	26.7	2.7
Cpx	1.9	6.5	0
Amp	40.2	12.0	0
Total mafic component	42.1	45.2	2.7
% garnet in mafic component	0.0	59.1	100
% clinopyroxene in mafic component	4.5	14.4	0
% amphibole in mafic component	95.5	26.5	0
Total points counted	225,280	256,000	51,200

Figure 8(a–d) show plots of modes for quartz, garnet, clinopyroxene and hornblende. Quartz and garnet are only found in the garnet reaction zone and the mode of each increases toward the garnet reaction zone/anorthositic vein boundary (Fig. 8a,b). Clinopyroxene is found as part of the S1 assemblage in the host gabbroic gneiss and as part of the garnet–clinopyroxene granulite assemblage in the garnet reaction zone. For the areas analysed, S1 clinopyroxene is <1 vol.% in the host gabbroic gneiss, whereas clinopyroxene becomes more than 6 vol.% in the garnet reaction zone. Figure 8(c) shows that this change is proportional to distance from the garnet reaction zone/host gabbroic gneiss boundary and increases away from it. The hornblende mode shows an antithetic trend to those of quartz, garnet and clinopyroxene (Fig. 8d). Figure 8(e–g) shows plots of the percentages of garnet, clinopyroxene and hornblende in the mafic component of the rock, which consists of approximately 65–70 vol.% garnet, 10–25 vol.% clinopyroxene and <20 vol.% hornblende. In the host gabbroic gneiss the mafic component is over 95 vol.% hornblende for sample 9814.

DISCUSSION

Garnet–clinopyroxene–rutile-bearing assemblages adjacent to D2 fractures and anorthositic veins cut S1 two-pyroxene hornblende assemblages in gabbroic gneiss of the Pembroke Granulite (Fig. 1). The formation of garnet granulite in gabbroic gneiss was related to an increase in pressure from conditions of $P<8$ kbar for $T=750$ °C at the time of S1 development to $P\approx14$ kbar for $T=750$ °C when the garnet reaction zones formed (Clarke *et al*., 2000). In the gabbroic gneiss, there is no consistent relationship between anorthositic vein thickness and the width of the associated garnet reaction zone, and the transformation to garnet reaction zone was largely isochemical. These observations are consistent with the anorthositic vein material having not been derived from garnet reaction zones in the gabbroic gneiss (*cf*. Oliver, 1977; Blattner & Black, 1980). Some D2 fractures, anorthositic veins and garnet reaction zones cut older D2 fractures, anorthositic veins and garnet reaction zones. This observation precludes interpretations involving the localisation of the garnet reaction zones and melt migration along a pre-existing fracture network (*cf*. Blattner, 1976; Oliver, 1977; Bradshaw, 1989c). The processes of rock fracturing, veining and garnet

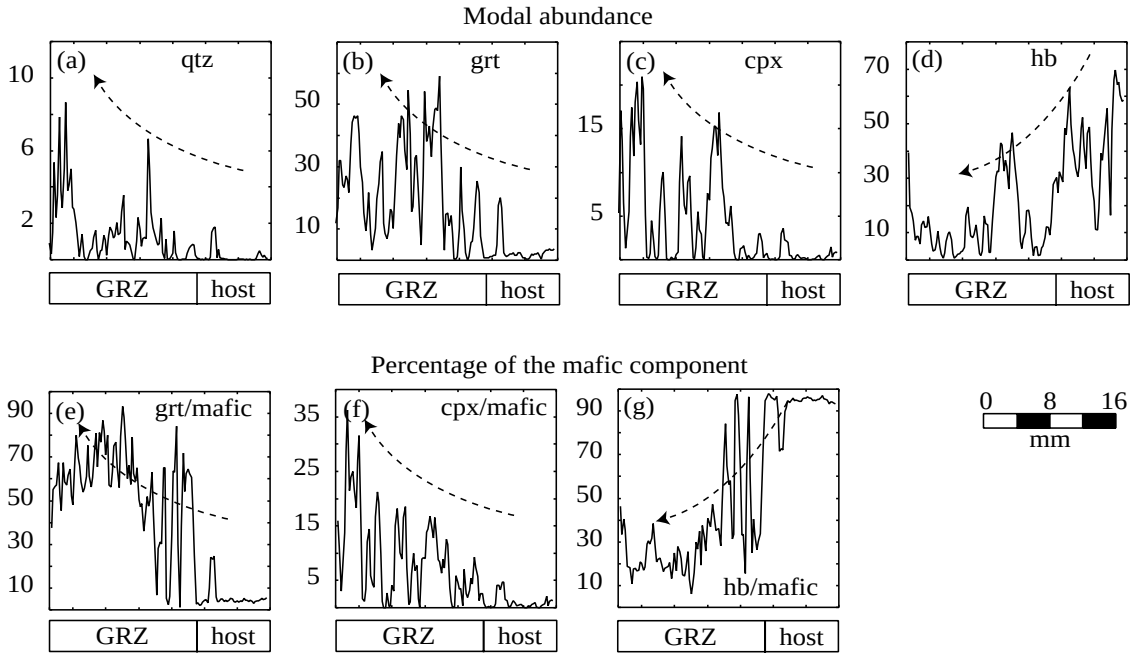

Fig. 8. (a)–(d) Plots of the change in modal abundance of quartz, garnet, clinopyroxene and hornblende across the garnet reaction zone (GRZ)/host gabbroic gneiss boundary for gabbroic gneiss sample 9814. Dashed lines with arrows represent the overall trend in the curves. (e)–(g) Plots of the change in the percentage of the mafic component of garnet, clinopyroxene and hornblende across the garnet reaction zone/host gabbroic gneiss boundary.

granulite formation were synchronous and repetitive in the gabbroic gneiss. The lattice pattern of D2 fracturing and veining indicates that brittle deformation accompanied the formation of the garnet reaction zones, when this belt of patchily recrystallized granulite was at crustal depths of approximately 45 km.

In the dioritic gneiss, post-S1 leucosomes that enclose idioblastic garnet and garnet trains indicate that this rock was partially molten. We infer that garnet was a peritectic product of a melt-producing reaction controlled by hornblende breakdown. Similar textures involving isolated patches of garnet-bearing leucosomes have been described from metapelitic granulites at Round Hill near Broken Hill (Powell & Downes, 1990), where limited nucleation of peritectic garnet is inferred to have localised the formation of melt segregations (Powell & Downes, 1990). Garnet-bearing leucosomes in the dioritic gneiss are continuous with garnet reaction zones and anorthositic veins in gabbroic gneiss (Fig. 2d), which is consistent with a causal relationship between the partial melting of the dioritic gneiss and formation of the garnet reaction zones in the gabbroic gneiss. Partial melting reactions commonly have a positive volume change and thus are a potential cause of embrittlement (e.g. Clemens & Mawer, 1992; Petford, 1995). If partial melting is to induce fracturing, the rate of the melt-producing reaction must be greater than the rate at which creep might accommodate the associated volume change (Connolly *et al.*, 1997). Connolly *et al.* (1997) demonstrated experimentally that reaction-induced microfracturing is a feasible mechanism of permeability enhancement during partial melting on regional metamorphic time scales. Therefore we infer that partial melting of the dioritic gneiss induced fracturing, in the presence of melt, which in turn greatly assisted melt segregation and the transition from distributed anorthositic leucosome to veins or dykes that cut gabbroic gneiss.

We suggest that partial melting in the dioritic gneiss is broadly similar to that determined experimentally for intermediate bulk compositions by Rutter & Wyllie (1988). These compositions undergo dehydration melting at lower temperature conditions than in mafic rocks, such as the gabbroic gneiss, at a given pressure (Rapp, 1995). Therefore we suggest that for a set T and P, partial melting in one rock may be concurrent with dehydration (involving no melting) in another. Therefore our model involves veining of gabbroic granulite by anorthositic melt at low a_{H_2O} and high-P. This led to vein-parallel desiccation, which manifests as loss of hornblende and gain of garnet–clinopyroxene, transforming a metastable medium-P ($P<8$ kbar) granulite into a high-P ($P=14$ kbar) garnet granulite in gabbroic gneiss.

The transition from two-pyroxene hornblende granulite to garnet–clinopyroxene granulite

The transition from two-pyroxene hornblende granulite to garnet granulite is restricted to garnet reaction zones in the gabbroic gneiss. The development of

garnet granulite assemblages involved the dehydration of S1 assemblages adjacent to the D2 fractures and anorthositic veins in the gabbroic gneiss. The replacement of S1 hornblende by garnet and clinopyroxene is most complete adjacent to the garnet reaction zone/anorthositic vein boundary, and gradually decreases away from this boundary. There is a clear physical and chemical link between the anorthositic veins in the gabbroic gneiss and the transition from two-pyroxene hornblende granulite to garnet granulite. Oliver (1977) and Blattner & Black (1980) inferred that the anorthositic veins were sourced from partial melting in the garnet reaction zones. However, the near-isochemical nature of the reaction zones preclude this possibility and partial melting in the dioritic gneiss is a more plausible source for the anorthositic veins. The observation of scapolite in some anorthositic veins led Blattner (1976) and Bradshaw (1989c) to propose that the introduction of CO_2-rich fluids along the D2 fractures and veins promoted the transition to garnet granulite in reaction zones adjacent to fluid pathways. However, garnet reaction zones are absent from the dioritic gneiss, despite anorthosite-filled fractures that localise the garnet reaction zones being continuous across boundaries of gabbroic and dioritic gneiss. As the garnet-bearing leucosomes are continuous across the boundaries and the garnet reaction zones are not, we prefer an interpretation involving the interaction of a low-H_2O melt with the gabbroic gneiss to form the garnet granulite. This interpretation is supported by an exception to the general isochemical pattern for the transition to garnet granulite established above, namely a doubling of Cu content in the garnet reaction zones (Cu≈19–20 ppm), compared to the Cu content of the adjacent host gabbroic gneiss (Cu≈11–12 ppm). As high trace amounts of Cu occur in the anorthositic veins (Cu≈25–50 ppm) and dioritic gneiss (Cu≈50–90 ppm), we infer that the additional Cu was introduced into the garnet reaction zones during interaction with anorthositic veins sourced from the comparatively Cu-rich dioritic gneiss. Further work on these textures could involve a study of trace elements in individual minerals to reveal which minerals controlled the sites of trace Cu. Finally, scapolite grains are restricted to the anorthositic vein material and possibly show igneous features. Elements (Cl, CO_3, SO_4, OH) needed for scapolite growth may have come from the breakdown of amphibole in the dehydration melting stage in the dioritic gneiss and in the garnet reaction zone stage in the gabbroic gneiss. This interpretation requires testing by *in situ* chemical analysis of hornblende and scapolite grains.

The transition from two-pyroxene hornblende granulite to garnet granulite has been studied in the mafic granulites of the Jijal complex of the Kohistan arc (Yamamoto & Yoshino, 1998). In this region, elongate patches and bands of garnet granulite transect a two-pyroxene host. Garnet-bearing veins are generally located in the middle of the reaction zones, similar to the Pembroke example. Geochemical studies of the Kohistan rocks indicate that this transformation was also essentially isochemical, but with Na_2O contents of the replacement rocks slightly lower than that of the host granulite. Yamamoto & Yoshino (1998) also inferred the loss of K_2O in some samples as a consequence of the transition and concluded that increasing pressure, along with infiltration of H_2O-poor and probably CO_2-rich fluid, was responsible for the replacement textures. The Kohistan arc example indicates that the vein-related transformation of two-pyroxene hornblende granulite to garnet granulite may be a common process related to the partial melting of lower crustal rocks.

Fracturing in the lower continental crust

The granulites that host the garnet reaction zones in the Pembroke Valley experienced elevated temperature conditions at comparatively deep crustal levels. The example described here indicates that partially molten, lower continental crust was able to fracture in a pattern similar to that of dyking in mantle peridotites underlying spreading ridges (e.g. Sleep, 1988). In both the Pembroke example and mantle peridotites, vertical dyking was followed or accompanied by ductile flow. However, the similarity of P–T conditions inferred from the garnet reaction zones and D3 mylonites (Clarke *et al.*, 2000; Daczko *et al.*, 2001) indicates that decompression did not induce melting and fracturing, unlike the mechanism controlling melting underneath spreading ridges. The products of incipient, incongruent melting in the dioritic gneiss of the Pembroke Granulite are centred on peritectic garnet grains, suggesting that garnet nucleation may have initially been a rate controlling step (Powell & Downes, 1990). Melt in low proportions was able to segregate, possibly into microfractures that have since been annealed. However, progressive melt accumulation around several garnet grains (Fig. 4) possibly involved a positive volume change and this initiated fracturing. The volume change associated with dehydration melting of amphibole $\pm$ biotite and clinozoisite is not well understood and requires further investigation. If the partial melting involved a positive volume change, this indicates that density-driven porous flow and filter pressing were not mechanisms controlling melt segregation for the Pembroke example. Instead we infer that dyke tapping (Sleep, 1988) or microfracturing (Connolly *et al.*, 1997) were the principal segregation mechanisms. Once in veins, melt would have migrated laterally into the gabbroic gneiss and almost certainly vertically.

As the water-poor anorthositic melt moved through the fracture system, we infer that it dehydrated the hornblende-rich wall rock of the gabbroic gneiss, activating the patchy and mostly isochemical change from two-pyroxene hornblende granulite to garnet-granulite. Fractures induced by dyke injection are

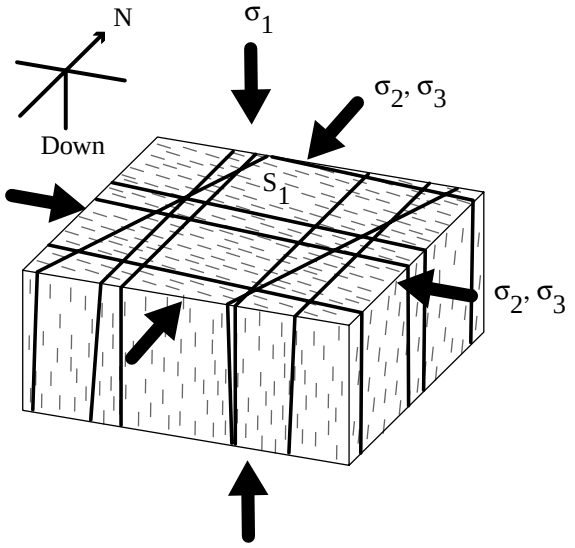

Fig. 9. Cartoon showing the orientations of the inferred ambient stress field during formation of the D2 fractures and associated garnet reaction zones. This represents a triaxial lithostatic stress field with the maximum principal stress vertical, consistent with the vertical orientation of the fractures

oriented normal to the minimum compressive stress (σ_3) and parallel to the maximum and intermediate compressive stresses (σ_1 and σ_2 respectively), as explained by Moores & Twiss (1995). The steeply dipping nature and planar angular relationships of the fractures and garnet reaction zones most probably reflect the late Cretaceous deviatoric stress field and indicate the terrain has undergone minimal body rotation (Fig. 9). We have no data to constrain how much melt was produced or how far melt moved vertically. Nonetheless, from the geometry of the veins, the scale of melt migration was probably larger than the observable rock area. The Pembroke example presents strong geological reasons for fracturing of the lower continental crust being a viable mechanism for the generation and initial ascent of felsic melt (Turcotte, 1982; Clemens & Mawer, 1992).

ACKNOWLEDGEMENTS

Funding to support this work was provided by Australian Research Council funding to KAK and GLC (grant number A10009053). An Australian Postgraduate Award supported NRD. We thank N. Mortimer and A. Tulloch of the IGNS, Dunedin for many helpful discussions and logistical assistance, and the Department of Land Conservation in Te Anau for permission to visit and sample localities in the Fiordland National Park. Thanks go to T. Patrick, J. Hollis and L. Turner for their enthusiastic assistance in the field. The editorial efforts of R.H. Vernon and critical reviews by N. Mortimer, G. J. H. Oliver and S.L. Harley considerably improved the paper.

REFERENCES

Bence, A. E. & Albee, A. L., 1968. Empirical correction factors for the electron microanalysis of silicates and oxides. *Journal of Geology*, **76**, 382–403.

Bishop, D. G., Bradshaw, J. D. & Landis, C. A., 1985. Provisional terrain map of South Island, New Zealand. In: *Tectonostratigraphic Terranes of the Circum-Pacific Region* (eds Howell, D. G., Jones, D. L. Cox, A. & Nur, A.), pp. 512–522. Circum-Pacific Council for Energy and Resources, Houston, Texas.

Blattner, P., 1976. Replacement of hornblende by garnet in granulite facies assemblages near Milford Sound, New Zealand. *Contributions to Mineralogy and Petrology*, **55**, 181–190.

Blattner, P., 1978. Geology of the crystalline basement between Milford Sound and the Hollyford Valley, New Zealand. *New Zealand Journal of Geology and Geophysics*, **21**, 33–47.

Blattner, P., 1991. The North Fiordland transcurrent convergence. *New Zealand Journal of Geology and Geophysics*, **34**, 553–542.

Blattner, P. & Black, P. M., 1980. Apatite and scapolite as petrogenetic indicators in granolites of Milford Sound, New Zealand. *Contributions to Mineralogy and Petrology*, **74**, 339–348.

Bradshaw, J. D., 1989a. Cretaceous geotectonic patterns in the New Zealand region. *Tectonics*, **8**, 803–820.

Bradshaw, J. D., 1993. A review of the Median Tectonic Zone: terrane boundaries and terrane amalgamation near the Median Tectonic Line. *New Zealand Journal of Geology and Geophysics*, **36**, 117–125.

Bradshaw, J. Y., 1989b. Origin and metamorphic history of an Early Cretaceous polybaric granulite terrain, Fiordland, southwest New Zealand. *Contributions to Mineralogy and Petrology*, **103**, 346–360.

Bradshaw, J. Y., 1989c. Early Cretaceous vein-related garnet granulite in Fiordland, southwest New Zealand: a case for infiltration of mantle-derived CO_2-rich fluids. *Journal of Geology*, **97**, 697–717.

Bradshaw, J. Y., 1990. Geology of crystalline rocks of northern Fiordland: details of the granulite facies Western Fiordland Orthogneiss and associated rock units. *New Zealand Journal of Geology and Geophysics*, **33**, 465–484.

Bradshaw, J. Y. & Kimbrough, D. L., 1989. Comment: Age constraints on metamorphism and the development of a metamorphic core complex in Fiordland, southern New Zealand. *Geology*, **17**, 380–381.

Brown, G. C., 1982. Calc-alkaline intrusive rocks: their diversity, evolution, and relation to volcanic arcs. In: *Andesites* (ed. Thorpe, R. S.), pp. 437–461. John Wiley, London.

Brown, E. H., 1996. High-pressure metamorphism caused by magma loading in Fiordland, New Zealand. *Journal of Metamorphic Geology*, **14**, 441–452.

Carter, R. M., Landis, C. A., Norris, R. J. & Bishop, D. G., 1974. Suggestions towards a high-level nomenclature for New Zealand rocks. *Journal of the Royal Society of New Zealand*, **4**, 5–18.

Clarke, G. L., Daczko, N. R. & Nockolds, 2001. A method for applying matrix corrections to x-ray intensity maps using the BENCE–AIREE.

Clarke, G. L., Klepeis, K. A. & Daczko, N. R., 2000. Cretaceous high-P granulites at Milford Sound, New Zealand: their metamorphic history and emplacement in a convergent margin setting. *Journal of Metamorphic Geology*, **18**, 359–374.

Clemens, J. D. & Mawer, C. K., 1992. Granitic magma transport by fracture propogation. *Tectonophysics*, **204**, 339–360.

Connolly, J. A. D., Holness, M. B., Rubie, D. C. & Rushmer, T., 1997. Reaction-induced micro-cracking: An experimental investigation of a mechanism for enhancing anatectic melt extraction. *Geology*, **25**, 591–594.

Daczko, N. R., Klepeis, K. A. & Clarke, G. L., 2001. Evidence of Early Cretaceous collisional-style orogenesis in northern

Fiordland, New Zealand and its effects on the evolution of the lower crust. *Journal of Structural Geology*, **23**, 693–713.
Gibson, G. M. & Ireland, T. R., 1995. Granulite formation during continental extension in Fiordland. *Nature*, **375**, 479–482.
Gibson, G. M. & Ireland, T. R., 1996. Extension of Delamarian (Ross) orogen into western New Zealand: Evidence from zircon ages and implications for crustal growth along the Pacific margin of Gondwana. *Geology*, **24**, 1087–1090.
Hill, E. J., 1995a. The Anita Shear Zone: a major, middle Cretaceous tectonic boundary in northwestern Fiordland. *New Zealand Journal of Geology and Geophysics*, **38**, 93–103.
Hill, E. J., 1995b. A deep crustal shear zone exposed in western Fiordland, New Zealand. *Tectonics*, **14**, 1172–1181.
Ireland, T. R. & Gibson, G. M., 1998. SHRIMP monazite and zircon geochronology of high-grade metamorphism in New Zealand. *Journal of Metamorphic Geology*, **16**, 149–167.
Kimbrough, D. L., Tulloch, A. J., Coombs, D. S., Landis, C. A., Johnston, M. R. & Mattinson, J. M., 1994. Uranium-lead zircon ages from the Median Tectonic Zone, New Zealand. *New Zealand Journal of Geology and Geophysics*, **37**, 393–419.
Kimbrough, D. L., Tulloch, A., Geary, E., Coombs, D. S. & Landis, C. A., 1993. Isotope ages from the Nelson region of South Island, New Zealand: structure and definition of the Median Tectonic Zone. *Tectonophysics*, **225**, 433–448.
Klepeis, K. A., Daczko, N. R. & Clarke, G. L., 1999. Kinematic vorticity and the tectonic significance of superposed mylonites in a major lower crustal shear zone, northern Fiordland, New Zealand. *Journal of Structural Geology*, **21**, 1385–1405.
Landis, C. A. & Coombs, D. S., 1967. Metamorphic belts and orogenesis in southern New Zealand. *Tectonophysics*, **4**, 501–518.
MacKinnon, T. C., 1983. Origin of the Torlesse terrane and coeval rocks, South Island, New Zealand. *Geological Society of American Bulletin*, **94**, 967–985.
Mattinson, J. L., Kimbrough, D. L. & Bradshaw, J. Y., 1986. Western Fiordland orthogneiss: Early Cretaceous arc magmatism and granulite facies metamorphism, New Zealand. *Contributions to Mineralogy and Petrology*, **92**, 383–392.
Moores, E. M. & Twiss, R. J., 1995. *Tectonics*. W.H. Freeman Co. New York.
Mortimer, N., 1995. Triassic to Early Cretaceous tectonic evolution of New Zealand terranes: a summary of recent data and an integrated model. In: *Proceedings of the 1995 PACRIM Congress, Australasian Institute of Mining and Metallurgy, Carlton, Victoria, Australia* (eds Mauk, J. L. & St George, J. D.), pp. 401–406.
Mortimer, N., Tulloch, A. J., Spark, R. N., Walker, N. W., Ladley, E., Allibone, A. & Kimbrough, D. L., 1999. Overview of the Median Batholith, New Zealand: a new interpretation of the geology of the Median Tectonic Zone and adjacent rocks. *Journal of African Earth Sciences*, **29**, 257–268.
Muir, R. J., Ireland, T. R., Weaver, S. D., Bradshaw, J. D., Evans, J. A., Eby, G. N. & Shelley, D., 1998. Geochronology and geochemistry of a Mesozoic magmatic arc system, Fiordland, New Zealand. *Journal of the Geological Society, London*, **155**, 1037–1053.
Muir, R. J., Weaver, S. D., Bradshaw, J. D., Eby, G. N. & Evans, J. A., 1995. The Cretaceous Separation Point batholith, New Zealand: granitoid magmas formed by melting of mafic lithosphere. *Journal of the Geological Society, London*, **152**, 689–701.
Muir, R. J., Weaver, S. D., Bradshaw, J. D., Eby, G. N., Evans, J. A. & Ireland, T. R., 1996. Geochemistry of the Karamea Batholith, New Zealand, and comparisons with the Lachlan Fold Belt granites of SE Australia. *Lithos*, **39**, 1–20.
Norrish, K. & Hutton, J. T., 1969. An accurate X-ray spectrographic method for the analysis of a wide range of geological samples. *Geochim. Cosmochim. Acta*, **33**, 431–453.
Oliver, G. J. H., 1977. Feldspathic hornblende and garnet granulites and associated anorthosite pegmatites from Doubtful Sound, Fiordland, New Zealand. *Contributions to Mineralogy and Petrology*, **65**, 111–121.
Oliver, G. J. H., 1990. An exposed cross-section of continental crust, Doubtful Sound Fiordland, New Zealand; Geophysical and Geological setting. In: *Exposed Cross-Sections of the Continental Crust* (eds Fountain, M. H. & Salisbury, D. M.), pp. 43–69. Kluwer Academic, Dorgrecht.
Petford, N., 1995. Segregation of tonalitic-trondhjemitic melts in the continental crust: The mantle connection. *Journal of Geophysical Research*, **100**, 15 735–15 743.
Powell, R. & Downes, J., 1990. Garnet porphyroblast-bearing leucosomes in metapelites: mechanism, phase diagrams, and an example from Broken Hill, Australia. In: *High Temperature Metamorphism and Crustal Anatexis* (eds Ashworth, J. R. & Brown, M.), pp. 105–123. Unwin & Hayman, London.
Powell, R., Holland, T. J. B. & Worley, B., 1998. Calculating phase diagrams with Thermocalc: methods and examples. *Journal of Metamorphic Geology*, **16**, 577–588.
Rapp, R. P., 1995. Amphibole–out phase boundary in partially melted metabasalt, its control over liquid fraction and composition, and source permeability. *Journal of Geophysical Research*, **100**, 15 601–15 610.
Rutter, M. J. & Wyllie, P. J., 1988. Melting of vapour absent tonalite at 10 kbar to simulate dehydration-melting in the deep crust. *Nature*, **331**, 159–160.
Sleep, N. H., 1988. Tapping of melt by veins and dikes. *Journal of Geophysical Research*, **93**, 10 255–10 272.
Turcotte, D. L., 1982. Magma migration. *Annual Review of Earth and Planetary Sciences*, **10**, 397–408.
Wandres, A. M., Weaver, S. D., Shelley, D. & Bradshaw, J. D., 1998. Change from calc-alkaline to adakitic magmatism recorded in the Early Cretaceous Darran Complex, Fiordland, New Zealand. *New Zealand Journal of Geology and Geophysics*, **41**, 1–14.
Williams, J. G. & Harper, C. T., 1978. Age and status of the Mackay Intrusives in the Eglinton-Upper Hollyford area. *New Zealand Journal of Geology and Geophysics*, **21**, 733–742.
Wood, B. L., 1972. Metamorphosed ultramafites and associated formations near Milford Sound, New Zealand. *New Zealand Journal of Geology and Geophysics*, **15**, 88–127.
Yamamoto, H. & Yoshino, T., 1998. Superposition of replacements in the mafic granulites of the Jijal Complex of the Kohistan Arc, northern Pakistan; dehydration and rehydration within deep arc crust. *Lithos*, **43**, 219–234.
Zen, E. A. N., 1986. Aluminium enrichment in silicate melts by fractional crystallisation: some mineralogic and petrographic constraints. *Journal of Petrology*, **27**, 2095–1118.

Received 5 May 2000; revision accepted 25 April 2001.